

Bipartite anchoring of SCREAM enforces stomatal initiation by coupling MAP Kinases to SPEECHLESS

Aarthi Putarjunan, Jim Ruble, Ashutosh Srivastava, Chunzhao Zhao, Amanda L. Rychel, Alex K. Hofstetter, Xiaobo Tang, Jian-Kang Zhu, Florence Tama, Ning Zheng, Keiko U. Torii

SUPPORTING INFORMATION

Figs. S1-S5

Fig. S1: SPCH protein is expressed in the absence and presence of SCRM. (Related to Fig. 1)

Fig. S2: Sequence alignment and interaction between SCRM_KiDoK-MAPK in homologs/orthologs of AtMAPK and SCRM respectively. (Related to Fig. 2)

Fig. S3: Representative phenotypes of additional transgenic lines expressing SCRM-KiDoK motif substitutions/deletions (Related to Fig. 3)

Fig. S4: Crystal structure of AtMPK6 and the CD domain of AtMPK6 (Related to Fig. 4)

Fig. S5: Superposition of AtMPK6 with ERK2 and sequence conservation of the substrate binding residue AtMPK6 E120 with animal MAPK orthologs (Related to Fig. 4)

Fig. S6: Secondary structure sequence alignment of AtMPK6 (Related to Figs. 4 and S4)

Fig. S7: Interaction analyses and Sequence alignment of substrate binding residues within AtMPK6 (Related to Fig. 4)

Fig. S8: Raw sensogram traces of *in vitro* substrate binding kinetics using the BLI ForteBio Octet Red System (Related to Figs. 2, 3 and 4)

Tables S1-S3

Table S1: Yeast two-hybrid screen and interactors (Related to Fig. 1)

Table S2: Statistics from crystallographic analysis (Related to Figs. 4 and S3)

Table S3: List of plasmids and primers

Table S4: Raw data of individual BLI experiments (Related to Figs. 2, 3, 4)

Table S5: Exact p values for statistical analysis (Related to Fig. 3)

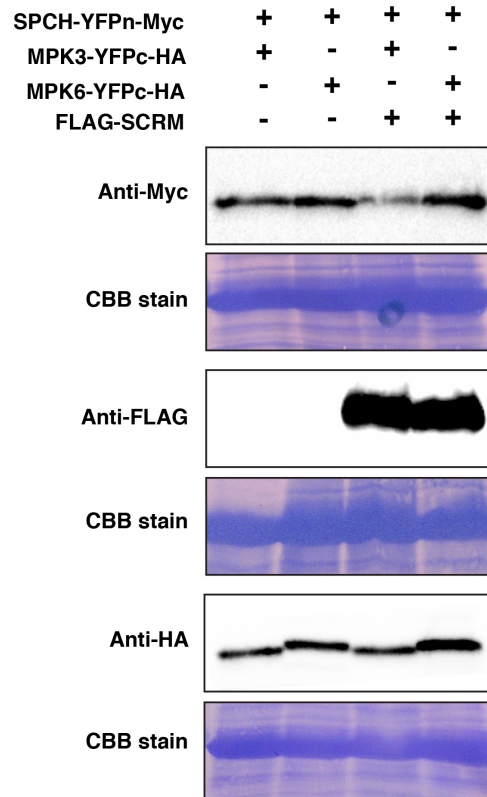


Fig. S1: SPCH protein is expressed in the absence and presence of SCRMs (Related to Fig. 1)

Shown are immunoblots for SPCH, SCRMs and MPK3/6 protein expression detected using Anti-Myc, Anti-FLAG and Anti-HA antibodies respectively from 3-week old *N. benthamiana* leaves agroinfiltrated using pairwise combinations of SPCH-YFPn-Myc and MPK3-YFPc-HA, MPK6-YFPc-HA along with 35Spro::FLAG-SCRMs. SPCH protein accumulates both in the absence and in the presence of the SCRMs protein, indicating that the absence of interaction between SPCH and MPK3/6 is not due to the SPCH protein not being expressed in the absence of SCRMs. CBB staining for each immunoblot is presented below the same. The experiment was repeated independently three times with similar results.

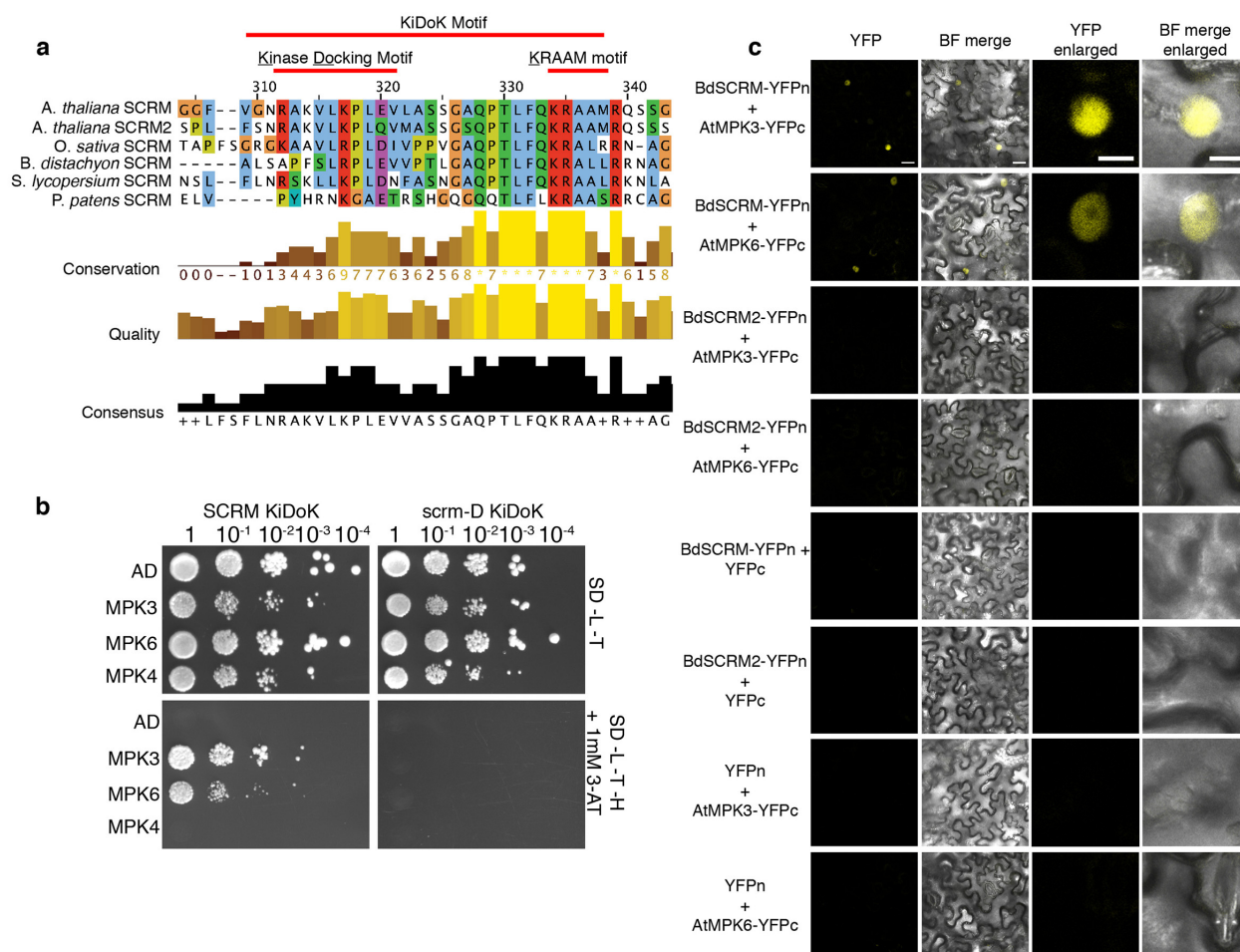


Fig. S2: Sequence alignment and interaction between SCRМ_KiDoK-MAPK in homologs/orthologs of AtMAPK and SCRМ respectively (Related to Fig. 2)

a, Sequence alignment of the SCRМ KiDoK motif in vascular as well as non-vascular plant orthologs of SCRМ created using JALVIEW. The KiDoK motif, which includes the Kinase Docking motif and the KRAAM motif, are highlighted using the red line above the motif.

b, Yeast two-hybrid (Y2H) assays of SCRМ-KiDoK and scrm-D KiDoK motifs with AtMPK3, AtMPK6 and AtMPK4. Bait constructs containing the wild-type KiDoK motif (SCRМ_KiDoK) and scrm-D version of the KiDoK motif (scrm-D_KiDoK) were tested in pairwise combinations with prey constructs containing the activation domain alone as well the activation domain fused to MPK3, MPK6 and MPK4. While MPK3 and MPK6 interact with SCRМ KiDoK motif and not the scrm-D KiDoK motif, MPK4 does not interact with both. The experiment was repeated independently three times with similar results.

c, Bimolecular Fluorescent Complementation (BiFC) assays. Shown are 3-week old *N. benthamiana* leaves agroinfiltrated with pairwise combinations of BdSCRМ-YFPn and BdSCRМ2-YFPn along with AtMPK3-YFPc and AtMPK6-YFPc. Scale bar = 25 μ m. Right two panels are magnified images of a representative nucleus. Scale bar = 10 μ m. While BdSCRМ associates with both AtMPK3 and AtMPK6 in the nucleus *in planta*, BdSCRМ2 that lacks the KiDoK motif does not. The experiment was repeated independently three times with similar results.

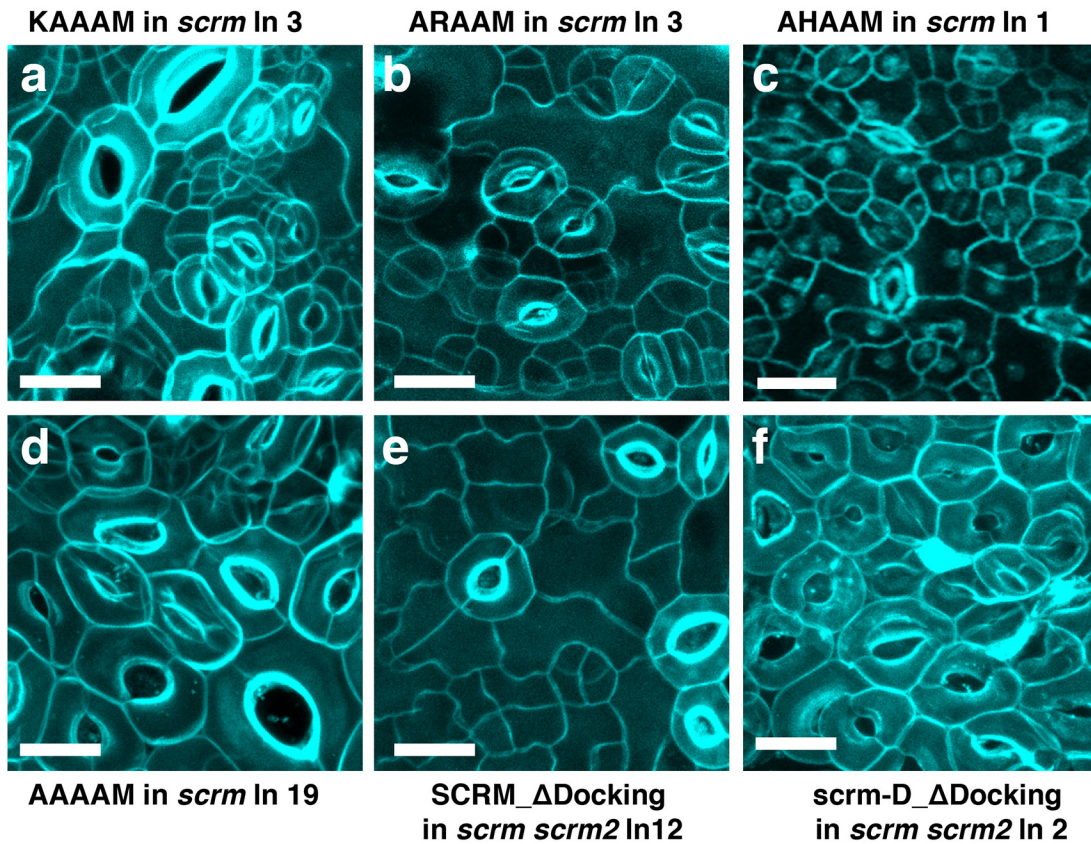


Fig. S3: Representative phenotypes of additional transgenic lines expressing the SCRМ-KiDoK motif substitutions/deletions (Related to Fig. 3)

Cotyledon abaxial epidermis phenotypes of 7 day-old additional transgenic lines of *Arabidopsis* seedlings expressing the SCRМ-KiDoK motif substitutions/deletions. **a**, *SCRМpro::SCRМ-KAAAM*; **b**, *SCRМpro::SCRМ-ARAAM*; **c**, *SCRМpro::SCRМ-AHAAM*; **d**, *SCRМpro::SCRМ-AAAAM* in the *scrм* background, and **e**, *SCRМpro::FLAG-SCRМ_ΔDocking* and **f**, *SCRМpro::FLAG-scrм-D_ΔDocking* in *scrм scrм2*. Scale bars = 20 μm. Each representative confocal image was obtained after imaging at least 2 independent frames from 3 seedlings for each genotype.

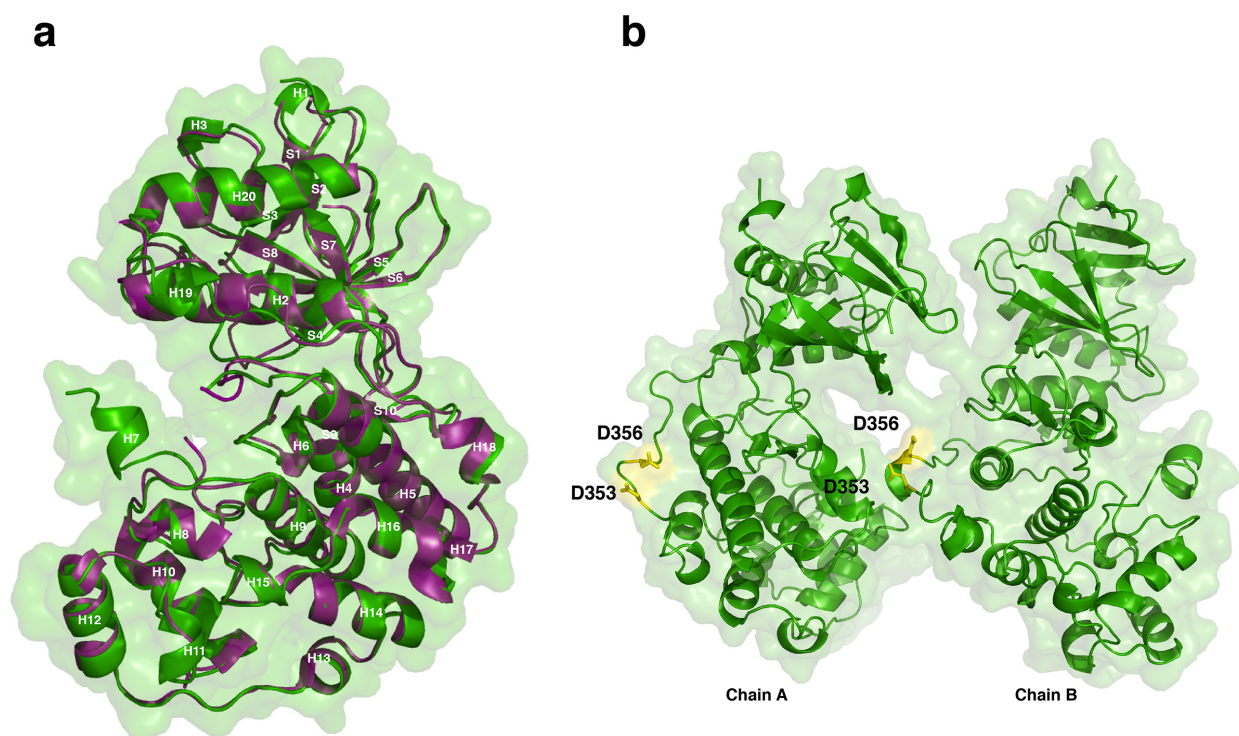


Fig. S4: Crystal structure of AtMPK6 and the CD domain of AtMPK6 (Related to Fig. 4)

a, Ribbon diagram superposition of the two MPK6 structures (green, this study PDB ID: 6DTL and magenta, PDB ID: 5CI6). MPK6 is composed of N-terminal and C-terminal lobes flanking a central ATP-binding region. Helices (H1-H20) are distributed between the N- and C-terminal lobes. Strands (S1-S10) are confined to the N-terminal lobe. The 6DTL includes an additional helical region, H7, comprising the phosphorylation loop proximate to the ATP-binding region.

b, Ribbon diagram of the MPK6 crystal structure dimer that houses two copies of MPK6 in the asymmetric unit of 6DTL. Shown in yellow are the exposed Asp residues of the CD domain of MPK6 (D353, D356).

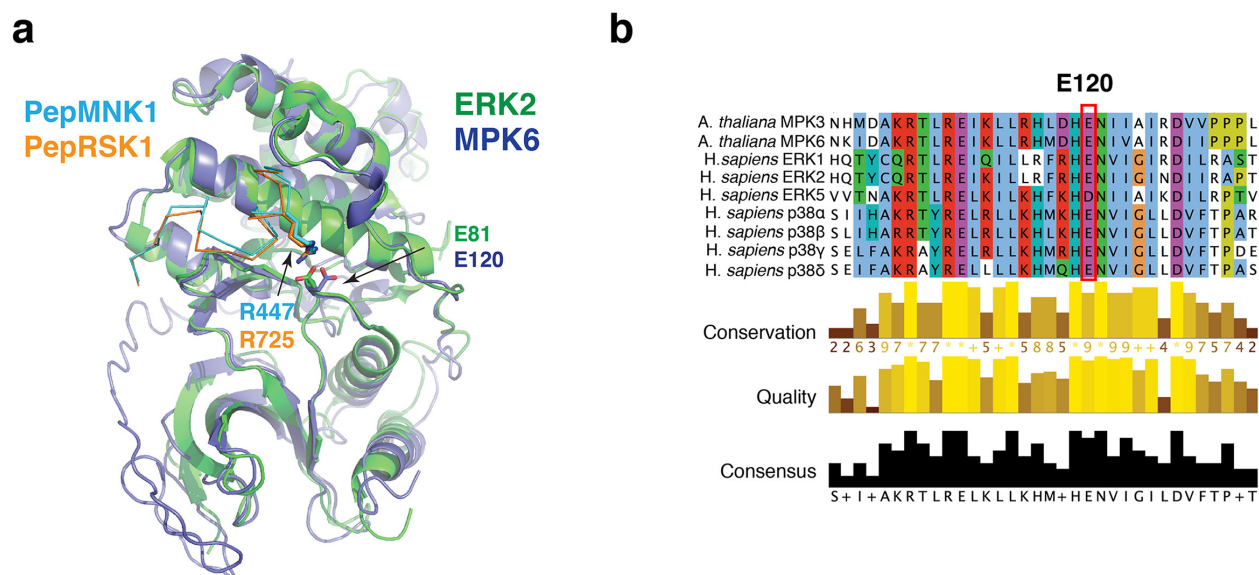


Fig. S5: Superposition of AtMPK6 with ERK2 and sequence conservation of the substrate binding residue AtMPK6 E120 with animal MAPK orthologs (Related to Fig. 4)

a, DALI search using AtMPK6 structure yielded ERK2 as the top hit with a Z score of 40.9. The two structures can be superimposed with an r.m.s.d of 0.71 Å over 260 Ca atoms. A superposition analysis of AtMPK6 (slate) with ERK2 (green) in complex with two individual substrate peptides (PepMKNK1 and Pep RSK1; PDB ID: 2Y9Q and 3TEI) predicts that AtMPK6 E120 should interact with a positive charged residue in the KiDock motif of SCRM, as ERK2 E81 does to contribute to substrate binding.

b, Sequence conservation analysis of the substrate binding residue E120 of AtMPK6 against animal MAPK orthologs (ERK and p38 family proteins) created using JALVIEW. While E120 of AtMPK6 is conserved amongst both plant and animal MAPKs.

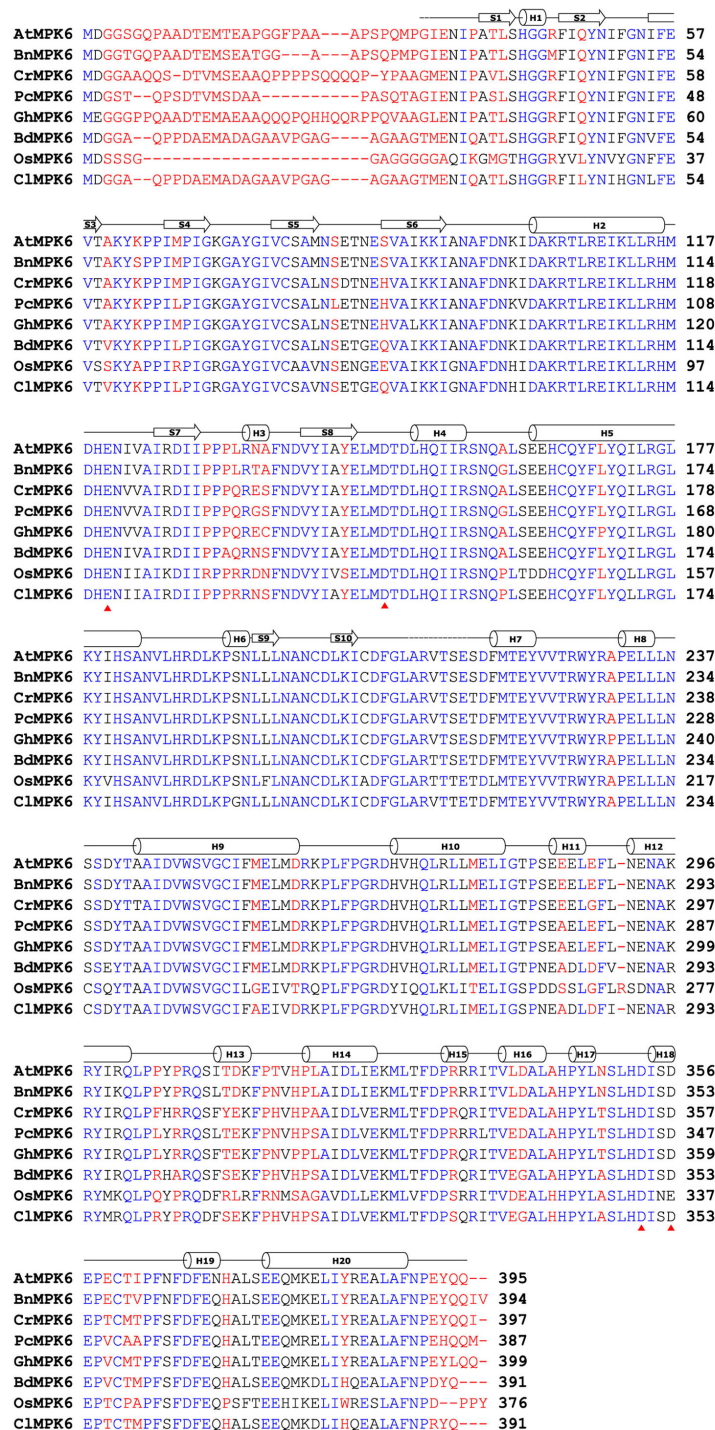


Fig. S6: Secondary structure sequence alignment of AtMPK6. (Related to Figs. 4 and S4)

Sequence alignment of the AtMPK6 along with its plant MPK6 orthologs. Secondary structure elements are depicted above the alignment (cylinder for α -helix and arrow for β -sheet). The exposed substrate binding residues on MPK6 (D148, E120, D353, D356) that are making contact with the SCRM KiDoK motif are depicted by red arrowheads.

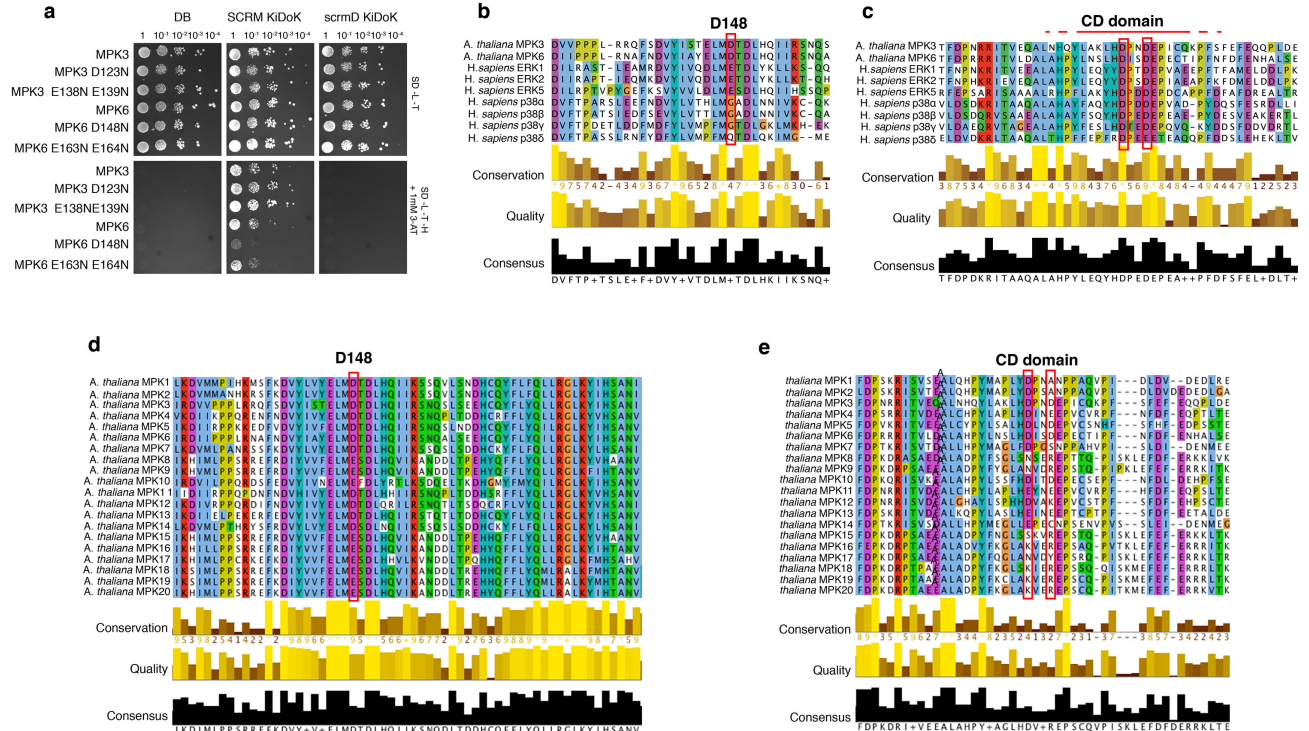


Fig. S7: Interaction analyses and sequence alignment of substrate binding residues within AtMPK6 (Related to Fig. 4)

a, Y2H assays of SCRM-KiDoK and scrm-D KiDoK motifs with potential exposed substrate binding residues on AtMPK6 (identified using ab-initio modeling) mutated to Asn. Bait constructs containing the wild-type KiDoK motif (SCRM_KiDoK) and scrm-D version of the KiDoK motif (scrm-D KiDoK) were tested in pairwise combinations with prey constructs containing the activation domain fused to MPK3, MPK3 D123N, MPK3 E138N E139N, MPK6, MPK6 D148N, MPK6 E163N E164N. Only MPK6 D148N showed severe reduction in interaction with the SCRM KiDoK motif, making D148 of MPK6 a substrate-binding site for the SCRM KiDoK motif. The experiment was repeated independently three times with similar results.

b, Sequence conservation analysis of the substrate binding residue D148 of AtMPK6 against animal MAPK orthologs (ERK and p38 family proteins) created using JALVIEW. D148 of AtMPK6 is far less conserved amongst animal MAPKs.

c, Sequence alignment of the CD domain of AtMPK3/6 with animal MAPK orthologs (ERK and p38 family proteins) created using JALVIEW. The exposed residues of the CD domain are highlighted using red boxes. The CD domain exposed residues of MAPK are highly conserved in both plant and animal systems.

d, e, Sequence conservation analysis of the substrate binding residues, D148 and D353, D356 of the CD domain of AtMAPK homologs (AtMPK1-20) created using JALVIEW. While D148 is highly conserved amongst all AtMAPK homologs, D353 and D356 of the CD domain of AtMPK6 are far less conserved amongst the other members of the AtMAPK family.

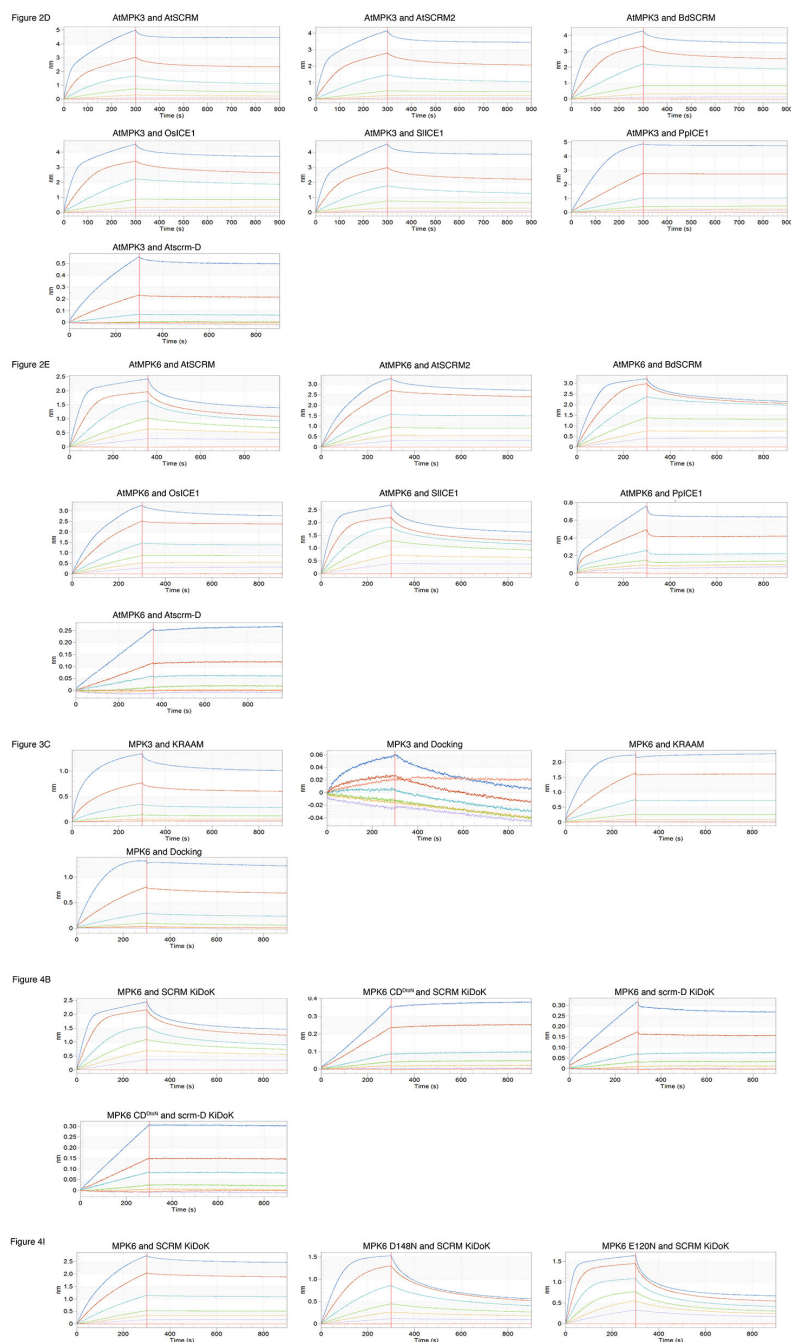


Fig. S8: Raw sensogram traces of *in vitro* substrate binding kinetics using the BLI ForteBio Octet Red System (Related to Figs. 2, 3 and 4)

Shown are representative raw sensogram traces of one (of three replicates) used in the *in vitro* binding kinetics experiments shown in Figs. 2,3 and 4. The 6 different concentrations used in every experiment are represented by blue, brown, cyan, green, yellow, purple and orange traces. Association with the peptide and protein was performed for the first 300 seconds followed by 600s of dissociation. The K_D values were calculated by fitting the association and dissociation curves with the 1:1 homogeneous ligand model. See Table S4 for the exact K_{on} , K_{dis} values for each experiment.

Table S2 Data collection and refinement statistics (molecular replacement)

Crystal 1: AtMPK6 Δ N	
Data collection	
Space group	P3 ₁ 21
Cell dimensions	
<i>a</i> , <i>b</i> , <i>c</i> (Å)	151.59, 151.59, 85.99
α , β , γ (°)	90.0, 90.0, 120.0
Resolution (Å)	50.00 – 2.75 (2.80-2.75) *
<i>R</i> _{sym} or <i>R</i> _{merge}	0.13 (1.35)
<i>I</i> / σ <i>I</i>	17.5 (2.04)
Completeness (%)	100 (100)
Redundancy	11.1 (10.6)
Refinement	
Resolution (Å)	42.98 – 2.75
No. reflections	27927
<i>R</i> _{work} / <i>R</i> _{free}	20.2/26.1
No. atoms	5929
Protein	5811
Ligand/ion	0
Water	118
<i>B</i> -factors	
Protein	43.1
Ligand/ion	0
Water	41.3
R.m.s. deviations	
Bond lengths (Å)	0.004
Bond angles (°)	0.71

*Values in parentheses are for highest-resolution shell.